Determination of the Optimum Docking Position for an Unmanned Underwater Vehicle using a Genetic Algorithm

Panagiotis Sotiropoulos, Nikos Aspragathos, Fivos Andritsos

***Abstract*— An approach for the determination of the optimum docking or hovering position of an Underwater Unmanned Vehicle is proposed towards the optimum performance for a desired intervention task. An underwater scenario with a UUV equipped with a 6 DOF manipulator is examined in order to verify the applicability of the algorithm. The optimization problem is formulated taken into account primarily the manipulator dexterity as well as the distance between the current position and the optimal one and the geometric constraints imposed by the environment. The ability of the vehicle to dock in the determined optimal location is assumed. A Genetic Algorithm is designed and implemented to search for the best docking position.**

Index Terms— Dexterous Manipulation, Genetic Algorithms, Optimization, Unmanned Underwater Vehicles.

I. Introduction

During the past few years underwater intervention operations have shaped a constantly growing field, mainly due to the demands of the hydrocarbon industry for the installation and maintenance of deepwater offshore sites. Search and recovery sector and research institutes of underwater archaeology could also benefit from these developments. Since divers even with the use of Atmospheric Diving Suits can operate only up to 700 meters, deep water interventions are performed mainly by Unmanned Underwater Vehicles (UUVs) equipped with manipulators, such as the currently operating Remotely Operated Vehicles (ROVs). The emerging Intervention Autonomous Underwater Vehicles (I-AUVs) could also provide a cost effective alternative in the near future. Some common underwater intervention tasks could be the manipulation of valves and switches on underwater facilities such as control panels on hydrocarbon underwater sites, the inspection and the maintenance, for example welding and cutting, on underwater structures and the object recovery and sampling from the sea bottom. In order to perform an intervention the vehicle has to temporarily dock or hover near the desired target point.

The determination of an appropriate docking position for the vehicle that could provide high dexterity configurations of the manipulator for an intervention task would minimize the possibility of a re-docking. This would imply less time to perform a task, shorter mission and thus cost reduction. Asokan has studied the optimum positioning of an underwater vehicle equipped with a manipulator to increase the efficiency on an underwater inspection task [1], noting that an inappropriate docking position would necessitate multiple re-dockings for the vehicle that would significantly increase the duration and the cost of the mission. For the special case of I-AUVs the avoidance of a re-docking would additionally mean energy savings that could lead to longer missions since energy capacity is limited. Moreover ensuring the dexterity of the manipulator arm from the vehicle's docking position to the tasks in hand prompts to faster manipulations and further time savings.

In order to quantify the manipulator's dexterity and provide singularity free work poses, several indices have been proposed for land robotic manipulators. Yoshikawa [2] proposed dexterity indices based on the kinematic and the dynamic manipulability ellipsoid of the manipulator in order to provide a quantitative measure of a robot's ability for manipulation inside its workspace. Aspragathos [3] proposed a globalised version of the Yoshikawa's manipulability index in order to determine the optimal location of a continuous path on the manipulator's workspace. Other indices have also been suggested such as the condition number of the Jacobian by Salisbury et al. [4] and the Manipulator Velocity Ratio (MVR) by Dubey et al. [5] as a measure of kinematic performance for the control of redundant manipulators. Also an index for the velocity efficiency for a robot moving its end-effector along a path based on the minimum MVR along it was proposed by Aspragathos and Foussias in [6].

Regarding the determination of the optimum base pose of a robotic manipulator several works have been presented, mainly for industrial, production line applications. The use of a genetic algorithm (GA) as the optimization method has been discussed in various papers. Mitsi et al. [9] proposed a method for determining the optimum robot base location using a hybrid genetic algorithm. Tien et al. [10] used a GA to define the optimum base location for a two-link planar manipulator.

Manuscript received July 13, 2010. This work was sponsored by the FREESUBNET program, Contract number MTRN-CT-2006-036186.

P. Sotiropoulos, is with the European Commission, Joint Research Centre, Ispra,VA 21027, Italy (Tel: 0039 0332785358 ; e-mail: panagiotis.sotiropoulos@jrc.ec.europa.eu).

N. Aspragathos, is with Mechanical Engineering and Aeronautics Department, University of Patras, Patras 26500, Greece (e-mail: asprag@mech.upatras.gr)

F. Andritsos, is with the European Commission, Joint Research Centre, Ispra,VA 21027, Italy (e-mail: fivos.andritsos@jrc.ec.europa.eu)

In this paper an algorithm that determines the optimum docking position for an UUV, equipped with a 6DOF robotic arm, performing an underwater intervention mission is presented. On the formulation of the objective function the manipulability index *w* of the arm, as defined by Yoshikawa [2], is considered as the measure of dexterity while the distance between the UUV's current position and the proposed docking point, and the specific geometric restrictions imposed by the environment are taken into account. A GA is implemented in order to solve the optimization problem and an underwater scenario that includes a grasping task is introduced for the demonstration of the method. The proposed algorithm provides a near-optimal docking pose for the vehicle. A number of test runs, in order to validate the applicability of the method, are presented in the Results section.

The paper is divided in the six following sections: *Introduction, Maximum Dexterity Docking*, *Optimization Problem*, *Results*, *Conclusions* and *Future Work*.

II. Maximum Dexterity Docking

The dexterity measures for manipulator arms describe their ability to move freely in all directions of their workspace. Manipulability measures are based on the Jacobian matrix of the arm that relates the joint velocities of the motors with the end-effector velocities. These measures describe the ability of the manipulator to change the position and orientation of its end-effector given configuration. Any singular configurations of the arm could be also indicated by the value of the dexterity measure.

In this work an algorithm is proposed that could later be embedded in the control system of the vehicle. The algorithm receives as input the pose of the vehicle relevant to the target and through an optimization process returns the docking pose assuring high dexterity for the manipulator from this point. Navigation towards a target point and the acquisition of the relevant vehicle's pose can be performed using acoustic or vision feedback. Evans et al. [7], described an autonomous docking system (ADS) for the ALIVE AUV, that was using sonar and video based real-time 3D pose estimation to control the vehicle while it was navigating relative to the docking panel. Krupinski et al. [8] proposed a visual model-based pose estimation using an on-board camera and active markers on the subsea structure to guide the vehicle during its docking face.

The underwater scenario examined in this paper consists of a grasping task that is to be performed by a hover-capable UUV after docking on a cement block that lays on the ocean bottom. The block can be traced easily and the vehicle can navigate towards it either by acoustic or visual feedback control. On the top side of the block there is a hook that is to be grasped by the vehicle. A depiction of the scenario appears in Fig. 1 when the UUV is approaching the block. The UUV is equipped with a 6-DOF elbow manipulator arm and is assumed that it can hover or dock on the determined optimal location. In order to dock firmly on the block a common suction cup or another equivalent method could be used.

The described task is inspired by the deployment procedure of the DIFIS (Double Inverted Funnel for Intervention on Ship Wrecks) [12] dome and a near optimum docking position as described before should be determined.

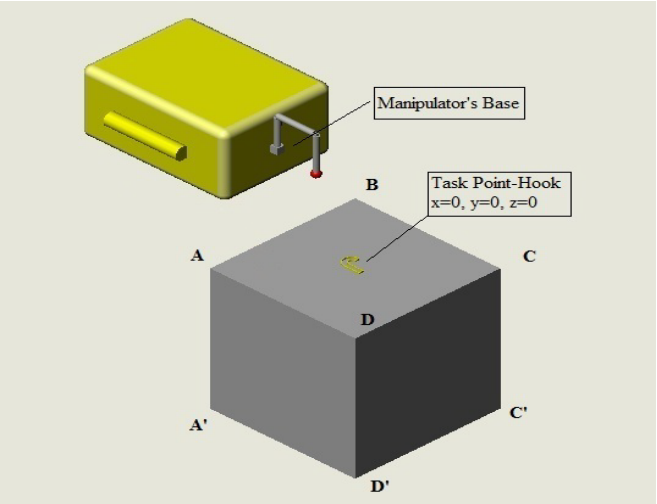

Figure 1: UUV approaching the block

III. Optimization Problem

A. Formulating the objective function

Certain terms that are used in the present section are defined and demonstrated in Fig.2.

The *global coordinate system {G}* is located in the middle of the top face of the block and the *manipulator's coordinate system {B}* is located at its base on the front side of the UUV as it is shown in Fig. 2.

The *guessed optimal pose* (^{G}p) indicates every candidate solution in the optimization problem and describes the manipulator's base. It is defined by $^{G}p=[x\ y\ z]$ the position vector of the base of the manipulator in *{G}* and ψ the rotation angle about the *z-axis* of the frame *{G}*.

The *proposed docking point* ($^{G}p_d$) is calculated according to each guessed optimal pose and refers to the vehicle's base where the suction cup is mounted. It is defined by $^{G}p_d=[\ ^{G}x_d\ ^{G}y_d\ ^{G}z_d]$ and indicated by the yellow star sign in Fig.2.

The *initial position of the manipulator's base* is given by $^{G}p_{init}=[\ ^{G}x_{init}\ ,\ ^{G}y_{init},\ ^{G}z_{init}]$ and the *initial position of the vehicle's base* is defined by $^{G}p_i=[^{G}x_i\ ^{G}y_i\ ^{G}z_i]$ and is indicated by the red star sign in Fig.2.

The *task point* is shown on the top of the block and it is given by the position vector $^{G}p_o=[x_o\ y_o\ z_o]$.

The UUV's base point, where the suction cup is mounted, is situated with respect to *{B}*, at $^{B}p_{bp}=[^{B}x_{bp}\ ^{B}y_{bp}\ ^{B}z_{bp}]$. It is demonstrated as the red disc on the bottom of the vehicle.

In the optimization process, every guessed optimal pose (^{G}p) is evaluated according to the objective function until the best one is found. The red sphere on the tip of the manipulator represents the last 3R.

As stated before the criterion for the optimality of a certain docking pose is Yoshikawa's manipulability measure. It is therefore calculated for every guessed optimal pose (^{G}p) such as the one depicted in Fig. 2.

ISBN: 978-988-17012-0-6
ISSN: 2078-0958 (Print); ISSN: 2078-0966 (Online)

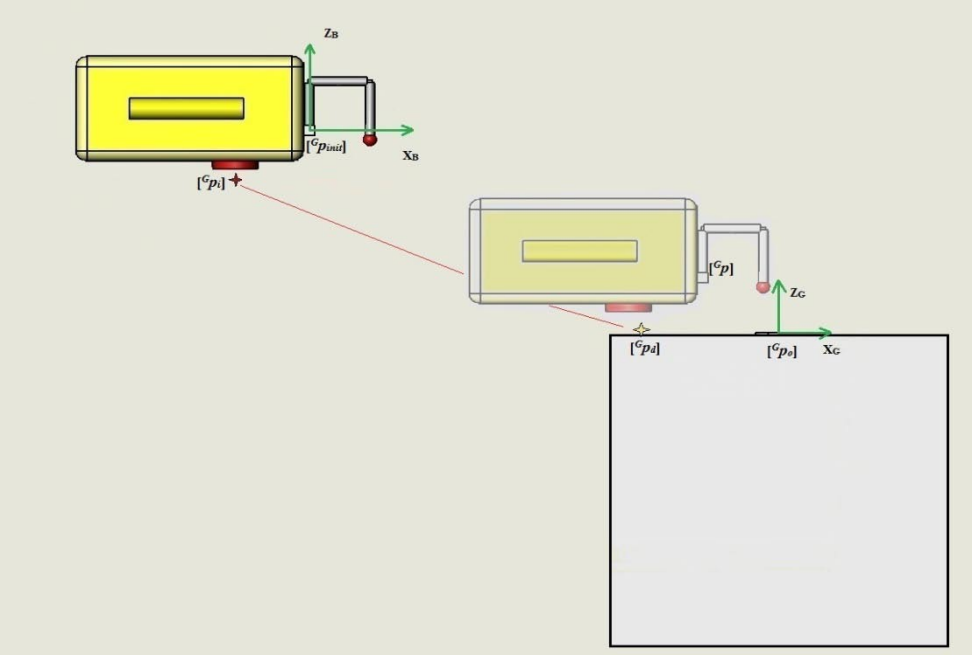

Figure 2: Side view of the vehicle and the block. Initial and proposed docking position

The manipulability measure for each pose is derived through the solution of the inverse kinematics problem and the calculation of the Jacobian matrix. The inverse kinematics solution is based on the Paden-Kahan sub-problems [11]. The manipulability measure is calculated according to:

$$w(\theta) = \sqrt{det\left(J\,(\theta)\,J^{T}(\theta)\right)} \tag{1}$$

where $J(\theta)$ is the Jacobian matrix, and the vector $\theta(x, y, z, \psi)$ is one of the possible joint configurations derived by the inverse kinematics solution for the considered pose.

It should be noted that for every single guessed optimal pose (^{G}p) there can be up to eight different solutions of the inverse kinematic problem, thus eight manipulability measures. The maximum of these is used for the calculation of the objective function.

On the formulation of the problem the manipulability measure is not the only factor considered. Since various, symmetrical poses on the block may be equally good candidates, a distance factor would serve on selecting the less expensive one in terms of distance to be covered by the vehicle. Hence the distance between the initial position of the base of the vehicle ($^{G}p_i$) and the proposed docking point ($^{G}p_d$) is taken into account. The Euclidean distance between these two points is demonstrated as a red line in Fig. 2 and is given by:

$$D = \sqrt{\left({}^{G}x_i - {}^{G}x_d\right)^2 + \left({}^{G}y_i - {}^{G}y_d\right)^2 + \left({}^{G}z_i - {}^{G}z_d\right)^2} \tag{2}$$

$^{G}p_i$ and $^{G}p_d$ are derived by the following transformations:

$$\begin{bmatrix} {}^{G}p_i \\ 1 \end{bmatrix} = {}^{G}To_B \cdot \begin{bmatrix} {}^{B}p_{bp} \\ 1 \end{bmatrix} \tag{3}$$

$$\begin{bmatrix} {}^{G}p_d \\ 1 \end{bmatrix} = {}^{G}T_B \cdot \begin{bmatrix} {}^{B}p_{bp} \\ 1 \end{bmatrix} \tag{4}$$

where $^{G}To_B$ is the homogeneous transformation matrix for the initial pose of the vehicle and $^{G}T_B$ is the homogeneous transformation matrix for the guessed optimal pose (^{G}p) given by:

$${}^{G}To_B = \begin{bmatrix} [R(\psi_{init})] & {}^{G}p_{init} \\ 0\,0\,0 & 1 \end{bmatrix} \tag{5}$$

$${}^{G}T_B = \begin{bmatrix} [R(\psi)] & {}^{G}p \\ 0\,0\,0 & 1 \end{bmatrix} \tag{6}$$

$R(\psi)$: is the *3x3* rotation matrix that defines the rotation along the ψ angle referenced to the global coordinate system *{G}*.
ψ_{init} is the initial angle of rotation of the vehicle about the *z-axis* of the frame *{G}*.

Summarizing, the optimization problem tackled here could be described as: *find the best docking position for the UUV given its initial pose and the target's position in order to ensure maximum manipulability*.
The objective function for this problem is given below:

$$f_{obj} = a \cdot M(w) - b \cdot D(x, y, z) \tag{7}$$

$M(w)$ is the manipulability measure function described as:

$$M(w) = \begin{cases} max(w_1, w_2, \ldots, w_8), if\ \theta_j^l < \theta_j < \theta_j^u, j = 1,..,6 \\ 0\ otherwise \end{cases} \tag{8}$$

where $w_i(\theta)$ is the manipulability measure for the i^{th} configuration of the manipulator as defined by (1) and $\theta=[\theta_1 \ldots \theta_j \ \ldots \ \theta_6\ ]$ the joint angles that are derived by the inverse kinematics solution for the current guessed optimal pose $[x, y, z, \psi]$. θ^l and θ^u are the limits for every joint.

ISBN: 978-988-17012-0-6
ISSN: 2078-0958 (Print); ISSN: 2078-0966 (Online)

a, b are weighting factors used to transform the two terms of the objective function to comparable amounts, since they may take different magnitude of values.

Last, it can be observed that the objective function is not continuous, due to the fact that for every single pose there exist multiple values for the manipulability measure and in the case that the joint angle limits are exceeded the manipulability value turns to zero. Thus the problem could not be solved with a simple gradient descent method and a GA is implemented to search for the optimum docking point.

B. The Genetic Algorithm

GA work in parallel to examine a number of initial points towards the search for the global minimum. In general, GA offer several advantages over other optimization methods, such as gradient methods, in the sense that they require only the objective function and not its derivative. They can find a near optimum solution even if the objective function is not continuous and they can perform robustly even in complex search spaces avoiding getting trapped in local minima. Also additional constraints could be easily specified inside the algorithm. In this particular problem the fitness function for the GA is equal with the objective function defined beforehand.

The constraints of the optimization variables are incorporated into the definition of the chromosome. Each chromosome consists of the *x*, *y* and *z* coordinates for its position and ψ Yaw angle for its orientation and it is represented as a binary chromosome of the form:

x	*y*	*z*	ψ
10…11	10…11	10…11	01…11

The length of every part of the chromosome depends on the range of field of values of each variable and the selected accuracy.

The field of values for the *x, y, z* coordinates is defined by the upper surface of the cube, adding a small margin *d* along the z-axis, where the final docking pose should be found. As a consequence the base point coordinates are bounded according to the following relations.

$$(x \geq x_A), (x \leq x_D) \quad (9)$$

$$(y \geq y_A)(y \leq y_C) \quad (10)$$

$$(z > z_A), \left(z \leq z_A + {}^{B}z_{bp} + d\right) \quad (11)$$

where ${}^{B}z_{bp}$ is the relevant z-axis distance between the manipulator and the vehicle's docking base and *d* is the small margin.

IV. Results

The cement block's and the UUV's dimensions in meters, along the x, y and z axis are, *2x2x2* (m) and *1.5x1.2x1* (m), respectively. The manipulator is a 6R with a spherical joint for the last three 3R. The lengths of the links are $lo=0.1m$, $l_1=l_2=0.4m$. The joints' angle limits are given in Table 1.

Table 1: Angle limits

Lower limit	*Angle*	*Upper limit*
-2.8	θ_1	2.8
-2.35	θ_2	2.35
-2.35	θ_3	2.35
-4.6	θ_4	4.6
-4.6	θ_5	4.6
-2.6	θ_6	2.6

A scheme of the manipulator on its zero angle configuration is demonstrated in Fig.3 below using Matlab's Robotic Toolbox [13]:

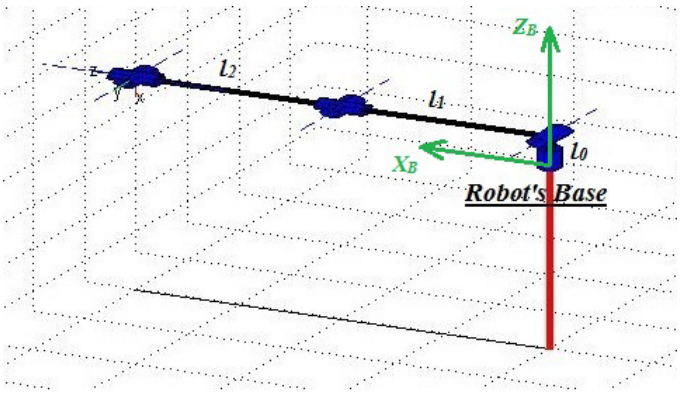

Figure 3: Manipulator at zero angle configuration

The vehicle's initial position is given by ${}^{G}p_{init}=[3\ 2\ 2]$ and the vehicle's base position relative to *{B}* is given by ${}^{B}p_{bp}=[-0.3\ 0\ -0.2]$.

Several runs were performed using the GA and the values for the algorithms settings have been fixed to the following:

Table 2: GA settings

Crossover Probability	*Mutation Probability*	*Population Size*	*Generations*
0.15	0.02	20	500

The results obtained from each run are a near optimum docking pose, its fitness function value and the manipulability measure. The results for several consecutive runs are demonstrated in Table 3.

After the acquisition of the poses, post process calculations are made to acquire the angles of every joint and are demonstrated in Table 4.

The configuration of the manipulator for the first and the second run is depicted in Fig.4 and Fig.5. In these figures the manipulability ellipsoid for each configuration is plotted in order to demonstrate the capability of movement of the manipulator's end-effector on the defined task point. It should be noted that the red line that appears in the figures is not part of the manipulator. It only indicates the projection of the centre of its base frame.

ISBN: 978-988-17012-0-6
ISSN: 2078-0958 (Print); ISSN: 2078-0966 (Online)

Table 3: Results

	x	*y*	*z*	*ψ*	*Fitness value*	*w*
1	0.111	0.559	0.242	-3.154	3.740	0.263
2	0.075	0.408	0.203	-3.042	3.432	0.234
3	0.039	0.544	0.241	3.034	3.715	0.258
4	0.297	0.187	0.226	-3.056	3.369	0.223
5	0.278	0.401	0.234	-3.101	3.749	0.264
6	0.226	0.458	0.211	-3.130	3.720	0.262
7	0.271	0.322	0.242	3.142	3.665	0.254
8	0.376	0.215	0.249	-3.180	3.701	0.255

Table 4: Joint angles

	θ1	*θ2*	*θ3*	*θ4*	*θ5*	*θ6*
1	1.379	-1.131	1.180	0	1.521	1.767
2	1.289	0.240	-1.747	0	-3.208	1.752
3	1.606	-1.195	1.274	-3.142	-1.493	-1.499
4	0. 478	0.180	-1.857	0	3.248	2.580
5	0.924	0.139	-1.478	0	2.910	2.177
6	1.100	0.179	-1.453	3.141	3.439	-1.112
7	0.863	-1.626	-1.642	0	-1.445	-0.851
8	0.558	-1.480	1.604	-3.142	-1.447	-0.519

Regarding the first three joints that define the position of the end-effector, two kinds of configuration occur as shown in the Fig 4 and Fig. 5. The configuration of the first kind (Fig.4) where the second and third joints have different signs from those of Fig.5, might cause collision of the manipulator on the block thus the second configuration would be preferable. To deal with this issue a motion planning part should be implemented in the method in order to avoid similar issues.

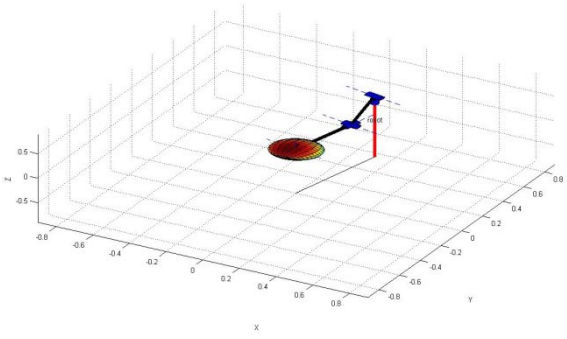

Figure 4: First pose configuration

From Table 4 it can also be observed that the manipulator's angles remain away from their limits. Especially the first three angles, that define the position of the end-effector, rest at a safe distance from their limits with high values for the second angle on the 5th and for the third angle on the 4th case where the limit is still respected though the value is relatively close to it.

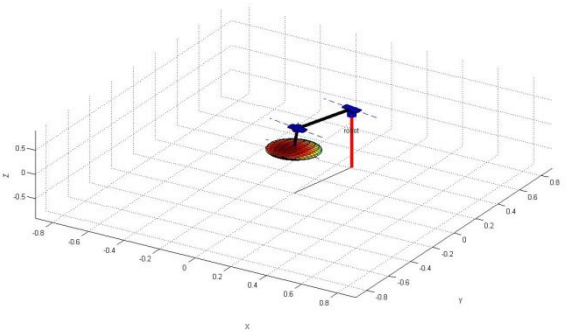

Figure 5: Second pose configuration

It should be noted that all the proposed docking poses lay on the same quarter of the upper surface of the cube, since it is the nearest to the predefined initial position. Though, it could be easily demonstrated that on the same quarter of the upper surface of the cube there exist also inappropriate poses for the manipulator's base, like the one depicted in Fig.6 that consists of:

x	*y*	*z*	*ψ*	*w*
0.491	0.464	0.213	-3.180	0.141

and its joint angles are:

θ1	*θ2*	*θ3*	*θ4*	*θ5*	*θ6*
0.796	-2.333	-0.749	0	-1.630	-0.757

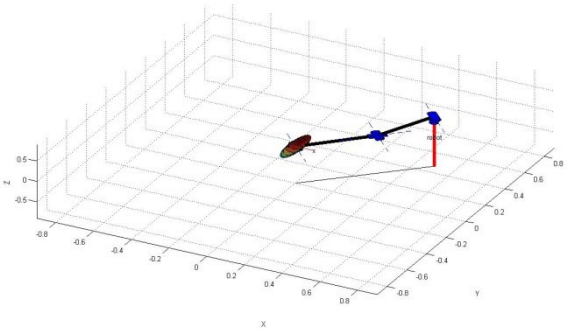

Figure 6: ill-placed docking pose

The low value for the manipulability measure indicates poor dexterity at the task point. It can be observed that the second angle is close to the joint limit and the manipulator will be constrained to move towards certain directions. On the manipulator's tips the ellipsoids of speed are demonstrated in Fig. 4, 5 and 6. It is obvious that for the last pose the ellipsoid's volume is significantly smaller according to its manipulability value. In addition the movement towards certain directions, such as the vertical axis in order to lift the hook, appears to be problematic for the same pose.

Nevertheless the GA in every run manages to avoid similar cases and to provide high dexterity poses for the manipulator's base.

ISBN: 978-988-17012-0-6
ISSN: 2078-0958 (Print); ISSN: 2078-0966 (Online)

V. Conclusion

In this paper an approach is introduced to determine the optimum docking position of an UUV equipped with a 6 DOF manipulator for an underwater intervention task. The GA implemented here received as an input the initial vehicle's position and the position of the block and returned a near optimum docking position on the block. The determined docking position assured high value of the manipulability measure on the task region while it was staying inside the margins set in order to dock on the top of the block. The proposed algorithm could be embedded in a UUV mission control system when intervention tasks are to be performed.

In this particular case the docking case examined imposed the suppression of the role and pitch angles, since the vehicle had to dock on the top of the block with its bottom side. The algorithm can easily be modified to deal with different cases were the vehicle has to dock on a vertical surface. In the case of a hover capable vehicle the docking position could be calculated in the same way simply by extending the chromosome and taking into account the Roll and Pitch angles.

VI. Future Work

Further work will follow on the motion planning for the manipulator in order to acquire collision free configurations. Moreover the actual introduction to a control system would provide an opportunity for further simulation or testing results. Last, further development of the algorithm is already under process.

References

[1] Asokan T. Seet G., Lau M. and Low E., Optimum positioning of an underwater intervention robot to maximize workspace manipulability, *Mechatronics*, Vol.15, pp.747-766, 2005

[2] Yoshikawa T., *Foundations of Robotics*, The MIT Press, Cambridge Massachusetts, 1990

[3] Aspragathos N.A., Optimal location of Path Following Tasks in the workspace of a Manipulator using Genetic Algorithms, Recent advances in Robot Kinematics, pp.179-188, 1996

[4] Salisbury J.K. and Craig J.J., Articulated Hands, Force control and Kinematic Issues, Int.J.of Robotics Research, No.1, pp.4-17, 1982

[5] Dubei R. and Luh J.Y., Redundant Robot Control Using Task Based Performance Measures, Robotic Systems Vol.5, No.5, pp.409-432, 1988

[6] Aspragathos N.A. and Foussias S., Optimal Location of a Robot path when considering Velocity Performance, Robotica 19, 2001

[7] Evans, J., Redmond, P., Plakas, C., Hamilton, K. and Lane, D., "Autonomous docking for Intervention-AUVs using sonar and video-based real-time 3D pose estimation," *OCEANS 2003. Proceedings* , vol.4, no., pp. 2201- 2210 Vol.4, 22-26 Sept. 2003

[8] Krupinski, S., Maurelli, F., Grenon, G. and Petillot, Y. , "Investigation of autonomous docking strategies for robotic operation on intervention panels," *OCEANS 2008* , vol., no., pp.1-10, 15-18 Sept. 2008

[9] Mitsi S., Bouzakis K.D., Sagris D. and Mansour G., Determination of optimum robot base location considering discrete end-effector positions, Robotics and Computer-Integrated Manifacturing, Vol.24, pp.50-59, 2008

[10] Tien L. and Collins C., Optimal placement of a two-link planar manipulator using a genetic algorithm, *Robotica*, Vol.23, Issue 2, pp.169-176, 2005

[11] Murray R.M. and Li Z., Sastry S.S., A Mathematical Introduction to Robotic Manipulation, CRC Press, New York, 1994

[12] Further information regarding the DIFIS project could be attained through the project's official website: http://www.ifremer.fr/difis/

[13] Corke P.I., A Robotics toolbox for MATLAB, *IEEE Robotics and Automation Magazine*, Vol.3, No.1, pp.24-32, 1996